Two interdependent mechanisms of antimicrobial activity allow for efficient killing in nylon-3-based polymeric mimics of innate immunity peptides ☆

Michelle W. Lee [a], Saswata Chakraborty [b], Nathan W. Schmidt [a], Rajan Murgai [a], Samuel H. Gellman [b], Gerard C.L. Wong [a,c,d,*]

[a] Department of Bioengineering, University of California, Los Angeles, CA 90095, United States
[b] Department of Chemistry, University of Wisconsin, Madison, WI 53706, United States
[c] Department of Chemistry and Biochemistry, University of California, Los Angeles, CA 90095, United States
[d] California NanoSystems Institute, University of California, Los Angeles, CA 90095, United States

ABSTRACT

Novel synthetic mimics of antimicrobial peptides have been developed to exhibit structural properties and antimicrobial activity similar to those of natural antimicrobial peptides (AMPs) of the innate immune system. These molecules have a number of potential advantages over conventional antibiotics, including reduced bacterial resistance, cost-effective preparation, and customizable designs. In this study, we investigate a family of nylon-3 polymer-based antimicrobials. By combining vesicle dye leakage, bacterial permeation, and bactericidal assays with small-angle X-ray scattering (SAXS), we find that these polymers are capable of two interdependent mechanisms of action: permeation of bacterial membranes and binding to intracellular targets such as DNA, with the latter necessarily dependent on the former. We systemically examine polymer-induced membrane deformation modes across a range of lipid compositions that mimic both bacteria and mammalian cell membranes. The results show that the polymers' ability to generate negative Gaussian curvature (NGC), a topological requirement for membrane permeation and cellular entry, in model *Escherichia coli* membranes correlates with their ability to permeate membranes without complete membrane disruption and kill *E. coli* cells. Our findings suggest that these polymers operate with a concentration-dependent mechanism of action: at low concentrations permeation and DNA binding occur without membrane disruption, while at high concentrations complete disruption of the membrane occurs. This article is part of a Special Issue entitled: Interfacially Active Peptides and Proteins. Guest Editors: William C. Wimley and Kalina Hristova.

© 2014 Elsevier B.V. All rights reserved.

1. Introduction

Over the past decade, the development and spread of antibiotic resistance has become a major global health risk. Each year in the United States, antibiotic-resistant infections affect over 2 million people and result in more than 23,000 deaths. The expenditures associated with these infections in terms of annual health care costs and productivity losses are estimated to be as high as $20 billion and $35 billion, respectively [1]. Most antibiotics in clinical use kill or inhibit the growth of metabolically active bacteria by targeting various biosynthetic processes in growing bacteria, including the synthesis of proteins, RNA, DNA, peptidoglycan, and folic acid [2–5]. For instance, the β-lactam class of antibiotics, which includes penicillins, cephalosporins, and carbapenems, inhibit cell wall synthesis in cells undergoing division. Aminoglycoside, macrolide, tetracycline, and other antibiotics target the bacterial ribosome to inhibit protein synthesis. Resistance can develop in at least two general ways: biomacromolecules targeted by an antibiotic can mutate to minimize or eliminate susceptibility (genetic antibiotic resistance), or bacteria can also adapt physiologically to become quiescent, or slow-growing. These persisting bacteria are able to evade deleterious effects through the down-regulation of biosynthetic processes that are often targeted by conventional antibiotics. Persisting bacteria are found in chronic infections, such as endocarditis, cystic fibrosis, and tuberculosis, which require prolonged treatment periods. Hence, there is a critical need for new structural classes of antibiotic

therapeutics that are effective against slow-growing cells, and are not impeded by mechanisms of antibiotic tolerance.

Antimicrobial peptides (AMPs) constitute a critical component of the eukaryotic innate immune system. Collectively, AMPs have broad-spectrum antimicrobial activity [6–11]. These host-defense peptides are diverse in sequence and structure, but two common features are cationic charge and hydrophobicity [8,9,12–15]. Some AMPs, such as cecropin and magainin, adopt an amphipathic α-helical secondary structure, in which cationic and hydrophobic side chains are spatially segregated from one another, upon interaction with membranes [8]. Other AMPs, such as bactenecin and defensins, feature antiparallel β-sheet structure, around which cationic and hydrophobic regions are segregated. The combination of hydrophobic and cationic subunits is believed to play a key role in the antimicrobial activity of AMPs, enabling the disruption of bacterial membranes through a combination of electrostatic interactions involving the cationic side chains with the anionic membrane along with the insertion of hydrophobic side chains into the nonpolar interior of the lipid membrane bilayer [8–10,16–18]. AMPs can destabilize membranes through a variety of processes, including pore formation, blebbing, budding, and formation of mixed peptide–lipid micellar assemblies ("carpet mechanism" [10]). Antimicrobial agents that mimic natural AMPs by targeting generic aspects of bacterial membranes may have potential for treating both antibiotic-resistant and slow-growing dormant infections. Membrane-disruptive antimicrobial agents that directly interact with the bacterial membrane bilayer can destabilize and compromise the physical integrity of the membrane. In general, membrane-targeted approaches have been shown to be clinically effective with newer antibiotics such as daptomycin, which is currently used to treat *Staphylococcus aureus* infections [2].

Recent work [7,19,20] has shown that the existence of negative intrinsic curvature lipids, such as those with phosphoethanolamine (PE) head groups, in the target membrane is an important determining factor in whether such membranes are permeated by AMPs: bacterial membranes with high PE concentrations are vulnerable to AMP-induced permeation, while eukaryotic membranes with low PE concentrations are not. Because many AMPs and synthetic compounds inspired by AMPs interact directly with membranes, the development of bacterial resistance against these agents is more difficult to achieve than against conventional antibiotics [21–24]. Nonetheless, bacterial resistance, in the form of reduced susceptibility to AMPs, is still possible through the modification of the membrane composition. Previous work has shown that bacteria can actively detect AMPs through two-component signal transduction systems, such as PhoQP in Gram-negative bacteria and GraSR in Gram-positive bacteria, and respond by altering their membranes [21,25–33]. However, a PE deletion, which would essentially confer immunity against membrane-active antibiotics, is found to be lethal in bacteria. This may help explain the unexpected absence of bacterial strains resistant to AMPs despite repeated exposure [19]. Thus, with increased clinical prevalence of bacterial resistance to conventional antibiotics, interest has grown in the prospect of using antimicrobial peptides as therapeutic agents, and in designing new antibiotics inspired by AMPs.

The attractive properties of natural AMPs have inspired extensive effort to develop synthetic analogues. Such efforts have included both oligomers of α-amino acids (α-peptides) [34–36] and oligomers that contain unnatural subunits, such as β-peptides [37–40], α/β-peptides [41,42], peptoids [43], and aromatic oligomers [44–48]. These AMP analogs have been demonstrated to provide various potential advantages over conventional antibiotics: (1) tunable, custom designs, (2) ease in preparation, (3) cost-effectiveness, (4) antibacterial potency with reduced likelihood of resistance, and (5) allowance for additional new built-in functions. In fact, recent work has highlighted quantitative differences between natural AMPs and their present synthetic analogs in terms of their hydrophobic content and cationic charge [49]. However, all unnatural AMP-mimetic oligomers have specific sequences of subunits, which require solid-phase synthesis, a technique that is costly

and therefore not practical for many applications [6]. This situation has prompted a number of groups to explore synthetic polymers as a novel source of AMP mimics over the past decade. In contrast to α-peptides and other sequence-specific oligomers, for which every molecule in a given sample is in principle identical, materials generated via polymerization reactions are mixtures, with variations in chain length and, for co-polymers, in subunit sequence. However, polymer production is much less expensive than production of sequence-specific oligomers. Early studies revealed that polymers with high intrinsic hydrophobicity could be effective against bacteria but not cell-type selective, since these materials are hemolytic [44,47,48,50]. More recently, polymers with carefully tuned hydrophobic-hydrophilic balance have been shown to match the generic AMP activity profile: inhibiting bacterial growth at low concentrations but causing hemolysis only at much higher concentrations [51–55]. Nylon-3 polymers have proven to be quite promising in this regard [51,53]. The nylon-3 backbone, comprised of β-amino acid residues, should be similar to the polyamide backbone of proteins in terms of physicochemical properties. Binary hydrophobic-cationic nylon-3 materials are readily prepared via anionic ring-opening polymerization of appropriate pairs of β-lactams [56].

In recent work, we have found that the bactericidal activity of a broad range of peptidic antimicrobials is correlated with the induction of negative Gaussian membrane curvature (NGC), also known as saddle-splay curvature, which enables membrane destabilizing processes such as pore formation, blebbing, and budding. All the membrane-active antimicrobials examined induce negative Gaussian curvature when the target membrane lipid compositions mimic those of bacterial membranes, but not when the lipid compositions are more representative of mammalian membranes. A key parameter for activity in this broad range of compounds is the concentration of negative intrinsic curvature ($C_0 < 0$) lipids, such as those with PE head groups, which exist at significantly higher concentrations in bacterial cytoplasmic membranes compared to eukaryotic membranes. Existence of homologous behavior in synthetic antimicrobials [19,20,57] suggests a common root mechanism for selective membrane permeation. In fact, the trends observed for antimicrobial-lipid interactions are consistent with killing assays using *Escherichia coli* mutants engineered to have different amounts of PE lipids in their cytoplasmic membranes [19]. Importantly, we have deduced a criterion for amino acid compositions of AMPs based on the requirement for generating saddle-splay membrane curvature, and we have shown that this criterion is consistent with trends in amino acid composition of 1080 known cationic AMPs [7].

Most biophysical studies of interactions between AMPs and membranes examine membrane behavior at a single lipid composition. However, bacterial membranes are known to exhibit different membrane compositions, which can be modulated in response to antimicrobials [58–65]. To complicate matters further, natural AMPs are intrinsically multifunctional. While many AMPs have membrane activity, it is known they also can bind intracellular targets [66–68] and have immunomodulating activities [6,69,70]. Due to these complications and others, it has been hard to correlate biophysical parameters, such as vesicle leakage and permeability, with antibacterial potency in general [9].

In this work, we examine a more circumscribed problem. We study the antimicrobial activity and membrane permeation activity of a set of nylon-3 polymers, including some that show AMP-like activity profiles. We show that this family of antimicrobial polymers is capable of two interdependent mechanisms of activity, one based on membrane permeation and one on DNA binding. Interestingly, at the minimal bactericidal concentration (MBC), the extent of bacterial membrane permeation, as measured by a β-galactosidase-based colorimetric assay on an *E. coli* ML-35 strain, is modest and clearly not enough to solubilize the entire membrane. All members of this family of antimicrobial polymers have sufficient local surface charge density to bind efficiently to intracellular DNA, in a manner similar to AMPs indolicidin [67] and buforin [68];

however, DNA binding cannot occur unless the polymer can traverse the bacterial membrane. We systematically investigate polymer-induced membrane deformation modes in a range of lipid concentrations found in *E. coli* and in mammalian cells using synchrotron small-angle X-ray scattering (SAXS). Our study includes three nylon-3 polymers with three compositions, tBuBz-MM$_{63}$CH$_{37}$ (**A**), Ac-MM$_{63}$CH$_{37}$ (**B**), and tBuBz-DM$_{50}$CH$_{50}$ (**C-1**, **C-2**, and **C-3**) (Fig. 1). Three different batches of the tBuBz-DM$_{50}$CH$_{50}$ polymer were used for these studies, designated **C-1**, **C-2**, and **C-3**. These batches differ slightly with respect to average chain length (n = 27, 25, and 21, and molecular weights of 5129, 4590, and 4018 Da for Polymers **C-1**, **C-2**, and **C-3**, respectively) and show highly similar activity profiles (see Supplemental Information). We find that the existence of NGC, which allows permeation of membranes and cellular entry of these antibacterial polymers in a manner reminiscent of cell-penetrating peptides, correlates well to their abilities to disrupt the membranes of and kill *E. coli*, a representative Gram-negative bacteria species [45–47]: polymers that have low minimum inhibitory concentrations (MICs) induce cubic phases rich in NGC, whereas polymers with high MICs do not induce such phases. While all of the nylon-3 polymers can bind to DNA, not all of them can permeate membranes, which explains their large observed range of MICs. Taken together, these results suggest that the nylon-3 polymers have a concentration-dependent mechanism of action. At concentrations near the MBC, they can permeate membranes without total membrane disruption and kill bacteria by binding intracellular targets such as DNA. However, at concentrations significantly higher than the MBC, they can potentially completely disrupt membranes. Furthermore, we find

the two-component mechanism of these polymers to be analogous to the mode of action employed by certain natural AMPs, such as indolicidin and buforin.

2. Material and methods

2.1. Polymer synthesis

Polymers were prepared from two types of β-lactam, some that lead ultimately to cationic subunits, MM ("monomethyl") or DM ("dimethyl"), and others that provide lipophilic subunits, CH ("cyclohexyl") [51,53,71,72]. All polymerizations were carried out in a N$_2$-purged dry box at room temperature. In a typical polymerization reaction, β-lactam monomers were weighed out in the appropriate molar ratio and placed in a reaction vial. To the vial was then added anhydrous THF and tbuBzCl or acetyl chloride (co-initiator) to achieve the desired monomer:co-initiator ratio and a monomer concentration of 0.1 M. The mixture was allowed to stir until all materials had dissolved. Polymerization was initiated by addition of Li(NSiMe$_3$)$_2$ solution (2.5 equivalent to the starting co-initiator concentration) in THF. The resulting solution was stirred for 3–4 hours at room temperature. The reaction vial was removed from glove box, and the polymerization was quenched by adding 3–4 drops of methanol. The resulting polymer was precipitated by pouring the solution into pentane. The solid was isolated by centrifugation, and the supernatant liquid was decanted off. The solid was re-dissolved in THF and then re-precipitated with pentane. After two more repetitions of precipitation/centrifugation procedure, the white
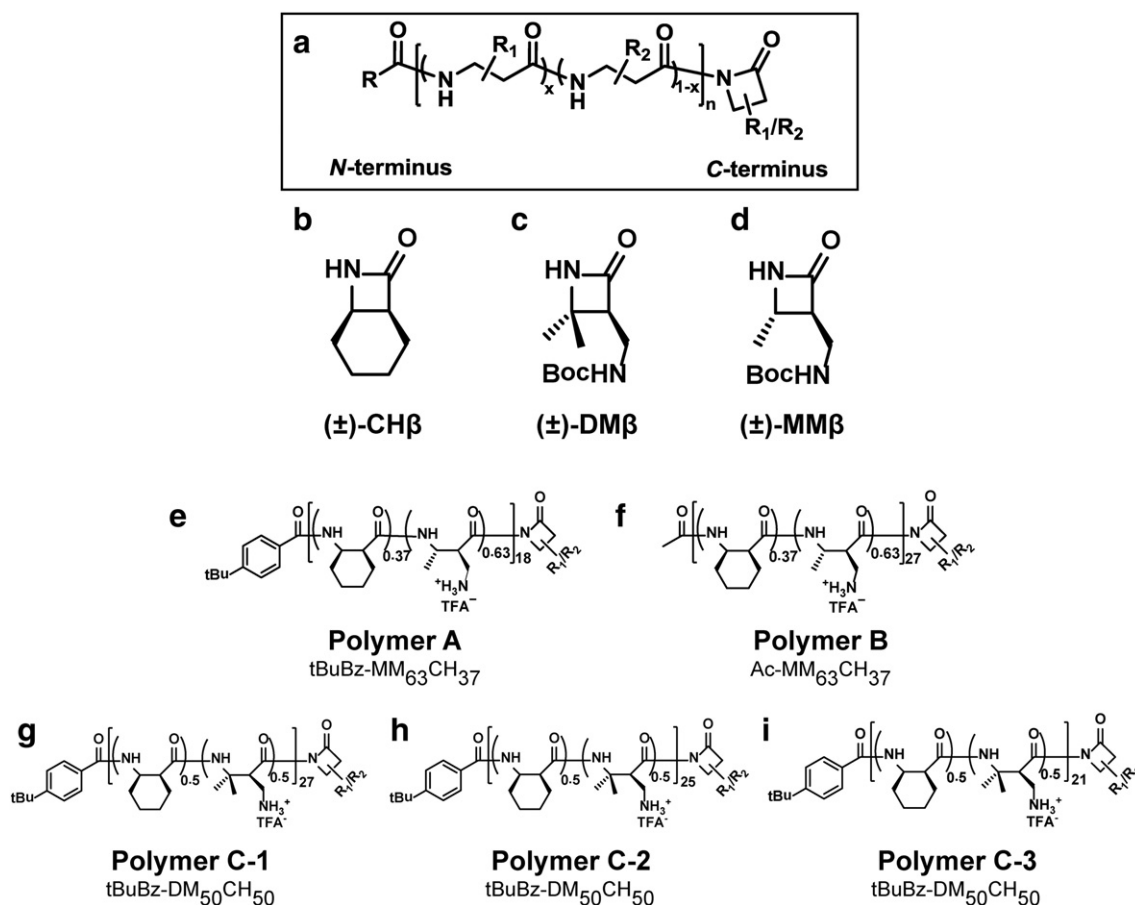

Fig. 1. Polymer structures. Sequence-random nylon-3 polymers of general structure (a) were synthesized using hydrophobic and cationic β-lactam monomers classified as CH (cyclohexyl), DM (dimethyl), and MM (monomethyl) (b–d). Because the monomers were racemic, the resulting polymers tBuBz-MM$_{63}$CH$_{37}$ (**A**), Ac-MM$_{63}$CH$_{37}$ (**B**), and tBuBz-DM$_{50}$CH$_{50}$ (**C-1**, **C-2**, and **C-3**) were heterochiral. In this study, we examine several representative members from these subfamilies (e–i). The C-terminal imide units on the polymer chains result from the β-lactam utilized in the polymerization, with R$_1$ and R$_2$ groups corresponding to the side chains of these β-lactams. Polymers have average chain lengths of 18, 27, 27, 25, and 21, and molecular weights of 3458, 5174, 5129, 4590, and 4018 Da for **A**, **B**, **C-1**, **C-2**, and **C-3**, respectively.

pellet was dried under vacuum to constant weight. Deprotection of the Boc group was carried out by dissolving the polymer in 2 mL neat trifluoroacetic acid. The reaction vessel was placed on a shaker for 2 hours (room temperature). The resulting solution was poured into cold ether to cause the deprotected polymer to precipitate. The solid was isolated by centrifugation, and the supernatant liquid was decanted off. The solid was dried under a stream of N_2. The precipitate was washed with ether twice and dried under vacuum. The material was then dissolved in 5–10 mL of water and lyophilized to yield the polymer as white fluffy solid.

2.2. Vesicle dye leakage experiments

Giant unilamellar vesicles (GUVs) composed of DOPS (1,2-dioleoyl-*sn*-glycero-3-phospho-L-serine (sodium salt))/DOPE (1,2-dioleoyl-*sn*-glycero-3-phosphoethanolamine)/DOPC (1,2-dioleoyl-*sn*-glycero-3-phosphocholine) = 20/60/20 were prepared encapsulated with 10 mM HEPES, 40 mM Calcein AM dye (pH 7). GUVs were synthesized using a freeze–thaw method and extruded through a 0.4 μm pore filter. The vesicles were then collimated and suspended in 100 mM NaCl, 10 mM MES buffer at a 1:12 dilution. A spectrofluorimeter was used to examine leakage in these vesicles, with excitation at 490 nm and emission at 510 nm. The baseline intensity of the vesicle solution was determined before polymer **C-1** solution was added in pre-determined polymer to lipid (P/L) molar ratios. The resulting increase in fluorescence intensity was indicative of vesicle leakage, and addition of 20% Triton X-100 was used to establish 100% leakage levels by fully permeabilizing the vesicle membranes. Percent leakage of calcein from vesicles was measured over a period of about 18 minutes. Polymer solution and Triton X-100 were added to vesicles at approximately 3 minutes and 16 minutes, respectively.

2.3. E. coli ML-35 membrane permeability assay

E. coli ML-35 strain was a generous gift from Professor André J. Ouellette at the University of Southern California. This particular *E. coli* strain is characterized by its lactose permease deficiency but constitutive β-galactosidase activity. Accordingly, it is unable to uptake the lactose analog *o*-nitrophenyl-β-D-galactopyranoside (ONPG) unless it is permeabilized by membrane-disruptive agents. Upon membrane permeation, ONPG diffuses into the bacterial cell cytoplasm and is hydrolyzed by β-galactosidase to yield *o*-nitrophenol (ONP), which can be measured by absorbance at 405 nm [73]. *E. coli* ML-35 cells were grown up in TSB at 37 °C for 18 hours to reach stationary phase. A 50 μL culture was diluted with fresh TSB by 100-fold and regrown at 37 °C for approximately 2 hours to reach mid-log growth phase, with an optical density (OD) at 600 nm of 0.5–0.7. Log-phase *E. coli* ML-35 cells were washed three times and resuspended in 100 mM NaCl, 10 mM MES (pH 7) to approximately 1×10^8 CFU/mL. In a 96-well plate, 15 μL of bacteria suspension was exposed to polymers (at specified concentrations) in the presence of 2.5 mM ONPG, 1% TSB, 100 mM NaCl, 10 mM MES (pH 7) for approximately 80 minutes at 37 °C. The kinetics of ONPG hydrolysis to ONP was measured by absorbance at 405 nm using a Tecan Infinite 200 microplate reader. Polymer **C-1** was assayed in quadruplicate for concentrations of 0, 10, 25, 50, and 200 μg/mL.

2.4. Minimum bactericidal concentration (MBC) assay

Frozen stock of *E. coli* DH5-α strain (Invitrogen) was streaked onto a fresh tryptic soy broth (TSB) agar plate and grown overnight at 37 °C. A single colony sourced from the streaked agar plate was used to grow up a new culture in TSB overnight in a 37 °C shaker. Bacteria from overnight culture was added to fresh TSB and shaken at 37 °C for 2 hours to achieve log-phase bacteria. *E. coli* was diluted down with additional TSB to a working density of ~5×10^6 CFU/mL. In a 96-well plate,

180 μL each of eight concentrations of polymer **C-1** solubilized in 100 mM NaCl, 10 mM HEPES (pH 7) was mixed with 20 μL of working bacteria solution, to achieve a total volume of 200 μL in each of the eight wells. Final concentrations of polymer **C-1** for these wells were 0, 1, 2, 2.5, 3, 3.5, 4, and 5 μg/mL. The plate was shaken at 37 °C for 1.5 hours. Reaction mixtures were then diluted 1:100 in 100 mM NaCl, 10 mM HEPES (pH 7); 100 μL of the each of the eight dilutions was plated onto TSB agar plates in 10×10 μL drops. Bacterial cell survival was determined by counting CFU after overnight growth at 37 °C and scaling up by the dilution factor, and expressed as a function of polymer concentration. The assay was completed in triplicate on the same day.

2.5. Liposome preparation for X-ray measurements

DOPS, DOPE, DOPC, DOPG (1,2-dioleoyl-*sn*-glycero-3-[phospho-*rac*-(1-glycerol)] (sodium salt)), and CL (bovine heart cardiolipin (sodium salt)), lyophilized lipids from Avanti Polar Lipids, were used without further purification. For X-ray experiments, small unilamellar vesicles (SUVs) were prepared by sonication. Individual lipid stock solutions of DOPS, DOPE, DOPC, DOPG, and CL were prepared in chloroform at a concentration of 20 mg/mL. Mixtures of these lipids were prepared at molar ratios. Chloroform was evaporated under N_2, and the lipid mixtures were further dried by overnight desiccation under vacuum. The dried lipid mixtures were resuspended the following day in 100 mM NaCl, 10 mM HEPES at pH 7, unless specified at pH 5 conditions (100 mM NaCl, 10 mM NaOAc), to a final concentration of 20 mg/mL. Aqueous lipid solutions were incubated at 37 °C overnight and then sonicated until clear. SUVs were obtained via extrusion of sonicated lipid solution through a 0.2 μm pore Nucleopore filter (Whatman).

2.6. λDNA preparation for X-ray measurements

Lambda DNA (1250 μg) was purchased from New England Biolabs; 40 μL of (refrigerator) chilled 3 M NaOAc and 5 μL of 0.3 M $MgCl_2$ were added into the λDNA vial. The mixture was then centrifuged at 4000 rpm for 1 minute at room temperature and cooled in the refrigerator for 20 minutes. A total of 800 μL of (freezer) chilled 100% ethanol was subsequently added to the mixture and then placed in the freezer overnight. The mixture was then centrifuged at 13,500 rpm for 10 minutes on the following day. The supernatant was removed and the precipitate washed by adding 1 mL of (freezer) chilled 100% ethanol and centrifuged at 15,000 rpm for 10 minutes at 0 °C. Supernatant was removed again and the precipitate was washed again, by adding 1 mL of (freezer) chilled 70% ethanol and centrifuged at 15,000 rpm for 2 minutes at 4 °C. The supernatant was removed and 70% ethanol wash was repeated. Once the supernatant was removed, the vial was inverted to drip dry onto filter paper for at least 2 hours. The λDNA was then reconstituted in 100 mM NaCl, 10 mM MES (pH 7).

2.7. Small-angle X-ray scattering experiments

Polymers and lipid solutions were mixed at specific P/L molar ratios and sealed in quartz capillaries (Hilgenberg GmbH, Mark-tubes). Samples were prepared in 100 mM NaCl, 10 mM HEPES at pH 7, unless indicated for pH 5 conditions (100 mM NaCl, 10 mM NaOAc). For λDNA samples, λDNA was mixed with polymer **C-3** at specified polymer to λDNA (P/D) charge ratios in 100 mM NaCl, 10 mM MES (pH 7) and sealed in quartz capillaries. SAXS experiments were conducted at the Stanford Synchrotron Radiation Lightsource (SSRL, BL 4-2) and at the Advanced Light Source (ALS, beamline 7.3.3), using monochromatic X-rays with energies of 9–11 keV and 10 keV, respectively. The scattered radiation was collected using a Rayonix MX225-HE detector (pixel size of 73.2 μm) at SSRL and a Pilatus 100k detector (pixel size of 172 μm) at ALS. No radiation damage was observed for the incident beam intensities and the exposure times used. 2D SAXS powder patterns were integrated using the Nika 1.50 package [74] for Igor Pro 6.31 and FIT2D [75].

2.8. SAXS data fits

Q positions of the diffraction peaks were obtained by visual inspection of the integrated scattering intensity I(Q) vs. Q SAXS data graphed in Origin Lab software. The ratios among these measured peak positions ($Q_{(hkl)\text{meas}}$) were compared with the ratios of permitted reflections for different crystal phases to identify the phases present in the sample. After determining the crystal phase, its lattice parameter was calculated by the slope of the linear regression through the set of points corresponding to the reflections, with each point designated by coordinates of $Q_{(hkl)\text{meas}}$ and the associated reflection (in terms of Miller indices, *h*, *k*, *l*). For a powder-averaged cubic phase $Q_{(hkl)\text{meas}} = (2\pi/a)\sqrt{(h^2 + k^2 + l^2)}$. We take the linear regressions of $Q_{(hkl)\text{meas}}$ vs. $\sqrt{(h^2 + k^2 + l^2)}$ for cubic phases, and from its slope ($m = 2\pi/a$), we can back out the cubic lattice parameters. SAXS data from λDNA samples were schematically represented using VMD software [96].

2.9. Bacterial growth inhibition (minimum inhibitory concentration (MIC)) assay

Assays were performed as previously reported with moderate changes in the procedure [39]. The bacteria used in these assays were *E. coli* JM109 [76], *Bacillus subtilis* BR151 [77], *S. aureus* 1206 (methicillin-resistant) [78], and *Enterococcus faecium* A634 (vancomycin-resistant) [79]. Antibacterial activities were determined in sterile 96-well plates. Bacterial cells were grown overnight at 37 °C on agar, after which a bacterial suspension of approximately 2×10^6 CFU/mL in Luria Bertani or Brain-Heart Infusion growth medium was prepared. Samples (50 μL) of this suspension were added to 50 μL of medium containing the polymer in 2-fold serial dilutions for a total volume of 100 μL in each well. The plates were then incubated at 37 °C for 6 hours. Bacterial growth was determined by measuring the OD at 650 nm using a Molecular Devices Emax precision microplate reader. Positive control was OD without addition of polymer and negative control was OD of the medium without inoculum. The MIC is defined as the lowest concentration at which complete inhibition of bacterial growth was observed (no increase in OD over the course of the experiment). Assays were performed in duplicate for two separate experiments.

3. Results and discussion

3.1. Nylon-3 polymer *C-1* demonstrates antimicrobial membrane activity through vesicle leakage, membrane permeabilization, and bactericidal assays

We examined the antimicrobial activity of polymer **C-1**, a member of the tBuBz-DM$_{50}$CH$_{50}$ subfamily, through lipid vesicle leakage, bacterial membrane permeation, and bactericidal activity experiments.

Vesicle leakage assay

We examined the membrane effects of polymer **C-1** with GUVs using fluorescence spectroscopy. GUVs of lipid compositions of DOPS/DOPE/DOPC = 20/60/20 mimicking PE-rich bacteria membranes were loaded with fluorescent calcein dye and incubated with polymer **C-1** at two polymer/lipid molar ratios: P/L = 1/28.3 and 1/56.7, which correspond to polymer concentrations of 1.99 and 0.995 μg/mL, respectively. Dye leakage was observed from the GUVs after exposure to the polymer, with higher P/L generating greater leakage (Fig. 2a). P/L = 1/56.7 reached maximum leakage of approximately 20% after 15 minutes exposure. P/L = 1/28.3, with twice the quantity of polymer, reached a maximum leakage of about 40% over the same amount of time. The leakage results demonstrate the ability of polymer **C-1** to permeabilize model bacteria membranes rich in negative intrinsic curvature lipids.
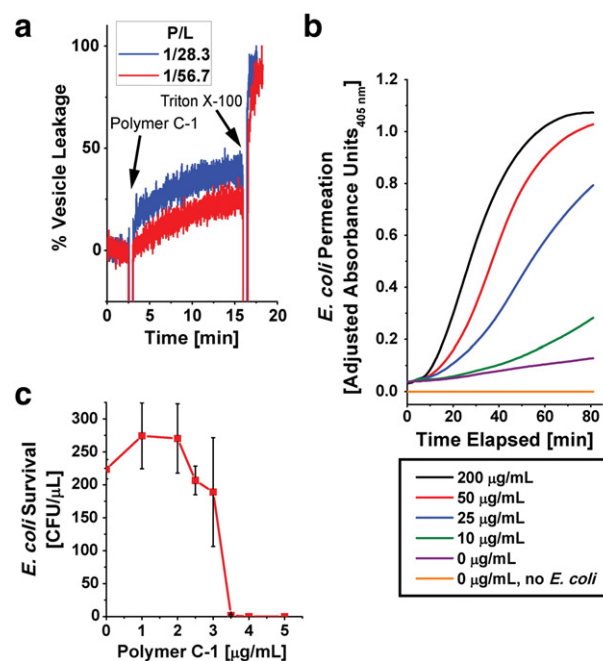

Fig. 2. Leakage, permeabilization, and bactericidal assays demonstrate polymer antimicrobial activity. Polymer **C-1** was shown to induce vesicle leakage, permeate *E. coli* membranes, and kill *E. coli*. (a) Polymer **C-1** was exposed to DOPS/DOPE/DOPC = 20/60/20 vesicles encapsulated with calcein dye at P/L ratios of 1/28.3 and 1/56.7, which correspond to polymer concentrations of 1.99 and 0.995 μg/mL, respectively. Percent leakage of calcein from vesicles was measured over a period of approximately 18 minutes. Polymer and Triton X-100 were added to vesicles at approximately 3 minutes and 16 minutes, respectively. (b) Polymer **C-1** was incubated with ML-35 *E. coli* to assess its ability to permeate bacterial membranes. Membrane permeation was assessed by the amount of ONP produced, which was measured with absorbance at 405 nm. Polymer **C-1** was added at approximately 3 minutes. The reported data are the average of four trials. (c) DH5α *E. coli* were exposed to polymer **C-1** to determine its bactericidal ability. MBC of polymer **C-1** was approximately 3.5 μg/mL for DH5α. Plot depicts the mean CFU/μL value at each polymer concentration. Error bars represent the standard deviation of the three trials.

Polymer-induced permeabilization of E. coli ML-35

To determine whether polymer **C-1** is able to permeabilize actual bacterial membranes and not just membrane vesicles with simplified lipid compositions, we conducted an inner membrane permeability assay using the *E. coli* ML-35 strain. We measured the β-galactosidase activity of *E. coli* ML-35 with ONPG as the substrate. *E. coli* ML-35 is lactose permease-deficient strain with constitutive cytoplasmic β-galactosidase activity. Therefore, *E. coli* ML-35 cannot hydrolyze the lactose analog ONPG unless cells are permeabilized by membrane-disruptive agents. Upon membrane permeabilization, ONPG diffuses into the *E. coli* cytoplasm. As a result, colorless ONPG is hydrolyzed by β-galactosidase and converted to ONP, which can be measured by absorbance at 405 nm. Thus, the level of absorbance corresponds to the level of permeabilization achieved by a membrane disruptive agent. (We note that permeation may exist via physical interactions between the polymer and membrane, at levels below those detectable in this type of assay.) Such membrane permeabilization assays have been previously utilized to assess the membrane destabilization capabilities of other nylon-3 polymers [52] and AMPs as well [80–83]. For this assay, we tested concentrations of polymer **C-1** up to 200 μg/mL in quadruplicate (Fig. 2b). Polymer was added at approximately 3 minutes. Increased absorbance was observed almost immediately upon addition of polymer **C-1** to the *E. coli* ML-35 cells, which suggests potent membrane destabilizing ability. Permeabilization kinetics were found to increase with increasing polymer concentration.

Bactericidal activity assays

To determine the lowest concentration of polymer **C-1** required to achieve bactericidal activity against the DH5-α strain of *E. coli*, an MBC assay was conducted. The experiment, completed in triplicate, evaluated polymer **C-1** over a range of eight concentrations, 0, 1, 2, 2.5, 3, 3.5, 4, and 5 μg/mL, with each assay consistently arriving at MBC ~3.5 μg/mL (Fig. 2c). These results show that polymer **C-1** has strong activity against *E. coli*.

Taken together, these results are all mutually consistent, and indicate that membrane permeation is a component of the antimicrobial activity of polymer **C-1**. A quantitative comparison between the results from the vesicle leakage, membrane permeabilization, and bactericidal assays is informative. Based on the results from the ML-35 β-galactosidase activity assay, the amount of membrane permeation is relatively modest at the MBC of ~3.5 μg/mL. This consideration suggests that the membrane has not been solubilized at the MBC, and that membrane permeation is responsible for only a part of the bactericidal activity of polymer **C-1**. We propose that another component of the polymer's antimicrobial effect arises from interaction with bacterial DNA.

Antibacterial nylon-3 polymers are highly cationic, with sufficient local surface charge density to bind to intracellular targets such as DNA, in a manner similar to AMPs indolicidin [67] and buforin [68]. An array of closely spaced cationic charges with a high charge density behaves much differently from the same number of cationic charges distributed farther apart. For instance, when a linear charged polymer has a distance between neighboring charged units of less than the Bjerrum length (~7 Å in water), Manning condensation will cause counterions to condense onto the charged polymer. Because of this phenomenon, the binding between cationic polymers and anionic polymers with similar local charge density is anomalously strong, due to the large entropic gain that results when the cationic and anionic surfaces charge compensate one another and release counterions maximally [84–87]. Using SAXS, we confirmed that the nylon-3 polymers we studied are capable of

strongly condensing DNA (see Supplemental Information), due to charge density matching. However, it is possible that other intracellular targets with similar charge densities can also be bound by the polymer. If we assume one copy of DNA per *E. coli* cell and complete charge matching between cationic polymer **C-1** and DNA, at the MBC of 3.5 μg/mL, we estimate that polymer **C-1** is able to condense up to 6×10^{-12} g of DNA per cell (see Supplemental Information). This quantity is ~1000-fold larger than the amount of DNA in a single *E. coli* cell [88]. Thus, at the MBC, 0.1% of polymer **C-1** molecules are sufficient to bind all DNA in the cell. Together these results suggest that the overall bactericidal activity of the nylon-3 polymers involve a combination of membrane permeation and DNA-binding activity. However, it is important to note that DNA binding cannot occur if the polymer is unable to cross the bacterial membrane, which we examine in the next section.

3.2. Sequence-random nylon-3 polymers can generate NGC in model bacteria membranes with high PE concentrations but not in model eukaryotic membranes with low PE concentrations

To investigate the membrane deformations induced by antibacterial nylon-3 polymers, we employed SUVs with phospholipid compositions representative of the Gram-negative bacterium *E. coli*, (DOPG/DOPE = 20/80). These SUVs were incubated with three polymers, **A**, **B**, and **C-2** (Fig. 1) at a variety of P/L ratios, and the resulting structures were characterized by SAXS. Synchrotron SAXS profiles (Fig. 3a–c) from lipid vesicle solutions exhibited a broad characteristic feature consistent with a single lipid bilayer form factor characteristic of unilamellar vesicles. When exposed to the nylon-3 polymer **A**, the lipid vesicles undergo a structural transition, as indicated by two distinct sets of new correlation peaks with specific ratios of Q values in the diffraction data (Fig. 3a). One set of characteristic Q-ratios $\sqrt{2}:\sqrt{3}$ indexed to the formation of a cubic (Q_{II}) *Pn3m* "double-diamond" lattice, with lattice parameter $a_{Q\_A} = 17.29$ nm (P/L = 1/57) (see Material and methods for indexing procedures). The other set had integral Q-ratios 1:2:3:4, consistent with a lamellar (L_{α}) phase having a lattice parameter $d_A \approx 5.18$ nm (across all tested P/L). When vesicles were exposed to **C-2**, we also observed two sets of correlation peaks (Fig. 3c). One set had Q-ratios $\sqrt{2}:\sqrt{4}:\sqrt{6}$,
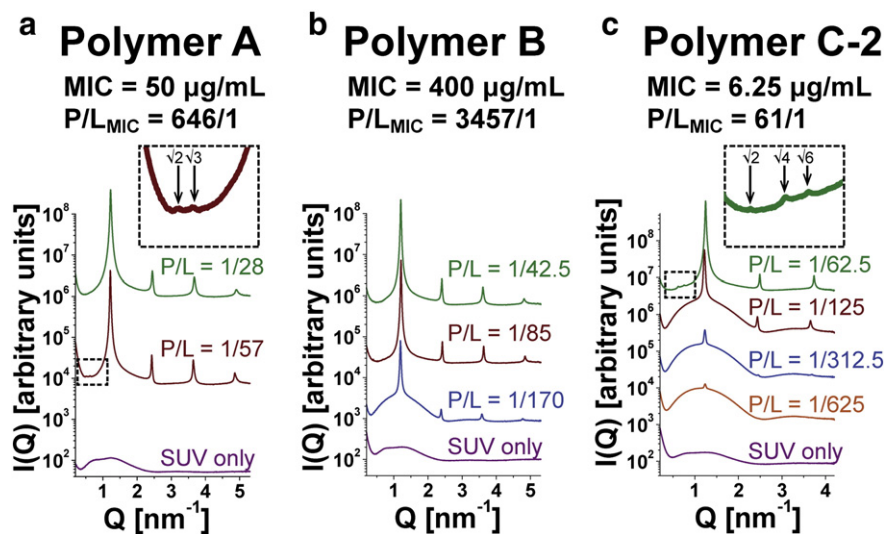

Fig. 3. SAXS spectra show polymer induction of NGC in prokaryotic-like membranes rich in PE. SAXS profiles from DOPG/DOPE = 20/80 lipid vesicle solutions after exposure to polymers **A**, **B**, and **C-2** (a–c). Correlation peaks indexing to the formation of a *Pn3m* cubic phase was observed for polymer **A** at molar ratio P/L = 1/57, which corresponds to a peptide to lipid charge ratio of 1. An *Im3m* cubic phase was induced when vesicles were exposed to polymer **C-2** at a molar ratio of P/L = 1/62.5, which also corresponds to a charge ratio of 1. In contrast to **A** and **C-2**, exposure of lipid vesicles to polymer **B** resulted in only a lamellar phase with a periodicity of 5.23 nm. The MICs and MIC-equivalent P/L molar ratio of each polymer are provided for comparison.
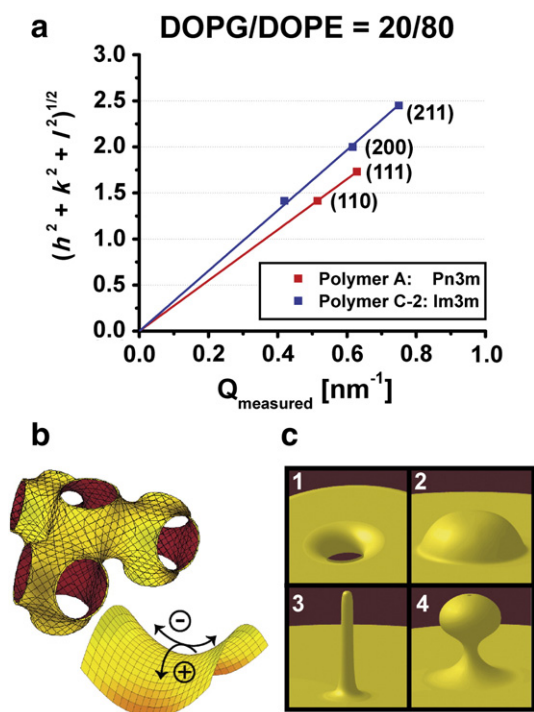
Fig. 4. Polymer-induced cubic phases are characterized by NGC. (a) The measured Q positions of the diffraction peaks were plotted for polymers **A** and **C-2** to show indexing of the cubic phases. The slopes of the linear regressions correspond to their lattice parameters, which were 17.29 nm and 20.59 nm, respectively. (b) A 3D illustration of the *Pn3m* cubic phase, which is characterized by negative Gaussian curvature at every point on the surface. Negative Gaussian curvature has a saddle-splay shape, with positive ($+$) curvature in one direction and negative ($-$) curvature in the perpendicular direction. (c) Negative Gaussian curvature can be found at the interior surface of a pore (1), the base of blebs (2) and rod-like projections (3), and the necks of buds (4).

indicating the presence of an *Im3m* cubic phase with lattice parameter $a_{Q\_C-2} = 20.59$ nm (P/L = 1/62.5), and the other had integral Q-ratios from a lamellar phase with lattice parameter $d_{C-2} \approx 5.10$ nm (across all tested P/L). In contrast to **A** and **C-2**, exposure of **B** to the lipid vesicles showed only a lamellar phase with a periodicity of $d_B \approx 5.23$ nm, indicative of inter-membrane attraction without the generation of significant curvature (Fig. 3b). The lattice parameters of each of the cubic phases were calculated by the slope of a linear regression through the set of points corresponding to the reflections, with each point defined by coordinates for the measured Q-position and its assigned reflection (Fig. 4a). Both the *Pn3m* and *Im3m* are bicontinuous cubic phases consisting of two sets of non-intersecting water channels separated by a lipid bilayer (Fig. 4b) [89,90]. The midplane of this bilayer traces a minimum surface characterized by NGC, also known as saddle-splay curvature, at every point. While bilayer saddle-splay curvature is distinct from self-connected monolayer saddle-splay curvature, such as that found in toroidal pores, each monolayer in a bicontinuous cubic phase is characterized by NGC at every point of the surface. NGC is the saddle-shaped curvature observed along the inside of toroids and at the bases of buds and blebs (Fig. 4c). Previously we found a strong correlation between AMP-induced formation of cubic phases and AMP-induced membrane permeation [7,91]. While both 2D membrane permeation (vesicle leakage and membrane permeabilization) and bulk 3D lipid system cubic phase generation (SAXS experiments) require NGC, the precise quantitative amount of NGC for each outcome is expected in general to be different. Our observations with model *E. coli* membranes show that two of the three nylon-3 polymers tested with SAXS, **A** and **C-2**, formed cubic phases, suggesting that these polymers may permeate membranes through the induction of NGC in a manner consistent with that of natural AMPs. The remaining polymer, **B**, does not appear to disrupt membranes due to the absence of cubic phases.
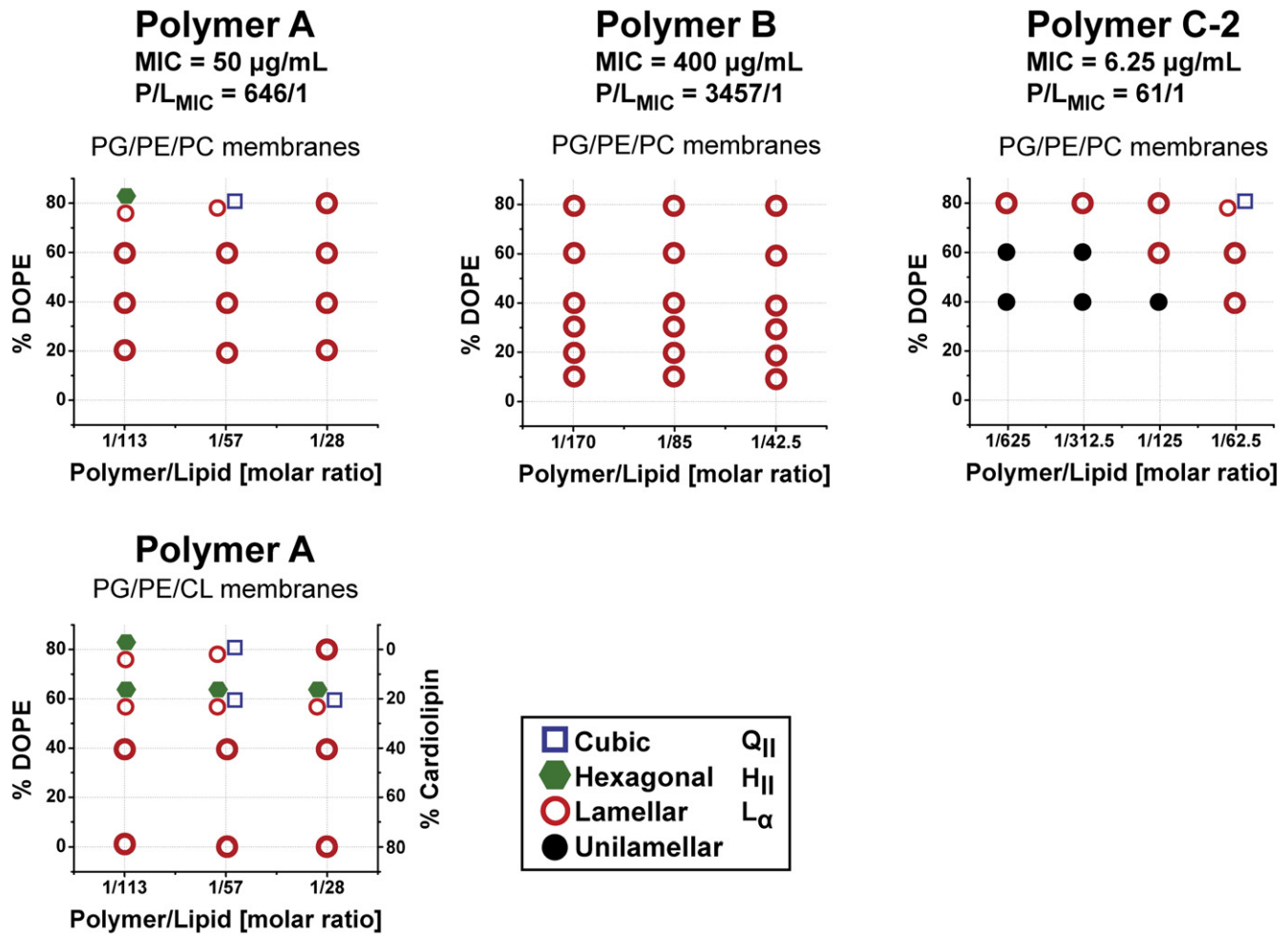
Interestingly, this observation is consistent with the MIC measured for **B**, as described below.

AMP selectivity against bacteria over animal cells is believed to be a consequence of their membrane compositional differences. Based on previous studies, amphipathic AMPs are believed to disrupt bacterial membranes through a combination of electrostatic and hydrophobic effects [6,8–10,16–18]. Bacterial membranes contain large amounts of anionic lipids such as PG, negative intrinsic curvature lipids such as PE, and also lipids such as CL that have both anionic and negative intrinsic curvature characteristics. These lipids are less common in the outer leaflets of animal cell membranes, which are rich in neutral zwitterionic lipids such as PC [7,8,16]. A range of lipid compositions have been reported for bacterial membranes [58–65]. To the origin of prokaryote vs. eukaryote selectivity of the nylon-3 polymers, we systematically examined how varying the membrane composition affects the ability of the polymers to restructure vesicles. We constructed SUVs with ternary DOPG/DOPE/DOPC lipid compositions with a constant anionic charge (DOPG = 20%) typical of bacterial membranes [92,93]. DOPG and DOPC are characterized by having zero intrinsic curvature ($C_0 \approx 0$), whereas DOPE and CL have negative intrinsic curvature ($C_0 < 0$). Enriching a membrane with these negative intrinsic curvature lipids will shift the monolayer intrinsic curvature toward more negative values. Thus, by fixing the DOPG content to 20%, we are able to independently tune the ratio of DOPE/DOPC and consequently membrane curvature. Phase diagrams for polymers **A**, **B**, and **C-2** (Fig. 5) illustrate that the general trend for decreasing DOPE/DOPC was the suppression of nonlamellar phase formation. More specifically, reduction of DOPE/DOPC membrane content to 60/20 extinguished the cubic phases, to leave only the lamellar phase. This observation further suggests that the nylon-3 polymers require high PE content of approximately 80% to generate NGC in lipid membranes. The phase diagram for polymer **A** at DOPG/DOPE/DOPC = 20/80/0 depicts a progression of inverted hexagonal phase (H_{II}) → Q_{II} → L_α as P/L increased to large values, with the induction of a cubic phase at a P/L charge ratio of ~1 (equivalent to molar ratio of P/L = 1/57). For an *E. coli* MIC assay, this P/L ratio of 1/57 corresponds to a polymer concentration of approximately 1.4 ng/mL (see Supplemental Information), which is drastically less than observed MICs as expected: structural changes in the membrane from NGC generation (such as pore formation) accumulate as the polymer concentration increases, and eventually culminate in the MIC.

Similarly, the phase diagram for polymer **C-2** indicates cubic phase generation at approximately the P/L charge ratio of 1 (molar ratio P/L = 1/62.5). Unlike the two previous polymers, **B** displayed only lamellar phases over the entire range of tested P/L ratios and membrane compositions. An additional set of ternary membranes of DOPG/DOPE/CL was tested with **A**, which also resulted in the generation of *Pn3m* cubic phases. For these lipid compositions, although we also observed nonlamellar phase suppression with decreasing DOPE/CL, cubic phases were induced at a lower PE content of 60%. This finding is consistent with previous studies that have shown that CL lipids can substitute for PE in certain conditions [57,94]. Because membrane lipid compositions vary between bacteria species and can undergo modification, we evaluated the robustness of curvature generation among a range of model membranes of different compositions. The preference for these nylon-3 polymers to generate cubic phases at a high PE content of 60–80% points to a mechanism of selectivity for bacterial membranes, such as that of *E. coli*, which has a composition of PG/PE/CL ≈ 20/70/10–20/75/5 [58,63]. We note that this mechanism is cognate with those observed for natural and synthetically derived AMPs [7,19,20,49,95].

3.3. Minimum inhibitory concentration (MIC) values of nylon-3 polymers against E. coli correspond with NGC generation observed in SAXS studies

Antimicrobial activity of polymers **A**, **B**, and **C-2** against *E. coli* was assessed by measuring their MICs. SAXS data collected previously on these nylon-3 polymers, with bacteria and eukaryotic-like model
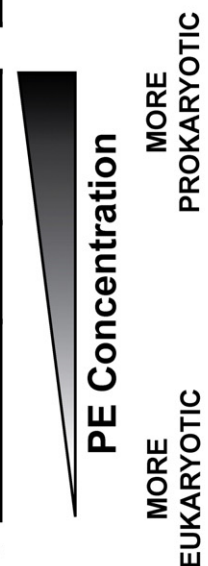
Fig. 5. MIC values of polymers against *E. coli* correspond with structural changes in model membranes. Phase diagrams of structural changes induced by polymers **A**, **B**, and **C-2** in ternary membranes composed of DOPG/DOPE/CL and DOPG/DOPE/DOPC with fixed DOPG content at 20%. Symbols used to indicate phases: open blue squares (Q_{II}), solid green hexagons (H_{II}), open red circles (L_α), and solid black circles (unilamellar). Table shows *E. coli* MICs and ability of each polymer to generate NGC in model membranes, with checkmarks indicating existence of cubic phases and Xs indicating their absence. The MICs and MIC-equivalent P/L molar ratio of each polymer are provided for comparison.

membranes, were compared against their MICs (table in Fig. 5). The five following compositions were used to model PE-rich prokaryotic membranes: DOPG/DOPE/CL = 10/80/10 and 20/60/20, DOPG/DOPE/DOPC = 20/80/0 and 20/60/20, and DOPS/DOPE = 20/80 [7,49,93]. The first three of these membranes served specifically to mimic that of *E. coli*, which is composed of PG/PE/CL ≈ 20/70-75/5-10 [58,63]. Membranes with decreased PE content served as eukaryotic-like models, which included the following: DOPG/DOPE/DOPC = 20/40/40, 20/30/50, 20/20/60, and 20/10/70. In general, we found that the presence of NGC, which allows for the permeation of membranes and cellular entry of these polymers, correlates to their bactericidal ability against *E. coli*. The polymers with low MICs (**A** and **C-2**) were able to induce cubic phases rich in NGC. However, polymer with a high MIC (**B**) was unable to induce cubic phases.

Polymer **A** induced cubic phases in the three membrane compositions that mimicked *E. coli*, which suggests that it destabilizes and permeates *E. coli* membranes by generating NGC. Its low MIC against *E. coli*, at 50 µg/mL, further supports the correspondence of induced membrane disruption with bacterial killing. Similarly, polymer **C-2** was observed to generate NGC in the *E. coli* model membrane DOPG/DOPE = 20/80 and had a potent MIC of 6.25 µg/mL. For **A** and **C-2**, there was diminished to no NGC generation for membranes that deviated from *E. coli* compositions. Because they exclusively induced NGC in compositions mimicking *E. coli* membranes, we can infer selectivity of these nylon-3 polymers for prokaryotic over eukaryotic membranes. On the contrary, recall polymer **B** induced only lamellar phases across the tested DOPG/DOPE/DOPC membranes. The absence of NGC generation suggests little to no membrane permeation. The high MIC value of 400 µg/mL for **B** further indicates low antimicrobial activity, which would result from the lack of both membrane permeation and DNA binding, the latter because this polymer is unable to traverse the cellular membrane.

We hypothesize that the lower antimicrobial activity and membrane activity of polymer **B** may be the result of an overall lower hydrophobicity in comparison with the other tested polymers, perhaps due to the absence of a *p*-(*tert*-butyl)benzoyl unit at the N-terminus and higher cationic charge resulting from 63% charged units of a longer chain length [53]. Lower hydrophobicity would decrease the tendency of the polymer to insert into the lipid core of membranes, which is necessary for permeation. Moreover, lower hydrophobicity and higher cationic charge of polymer **B** are in agreement with its decreased antimicrobial activity based on previously established design principles for AMPs [7].

4. Conclusions

We have demonstrated that the antibacterial activity of nylon-3 polymers can be attributed to two interdependent channels of action. These polymers are able to permeate bacterial membranes and to bind to intracellular targets such as DNA. The bactericidal activity of these polymers can be further correlated with their ability to generate cubic phases rich in NGC, which is topologically necessary for membrane-disruptive processes. Ablation of membrane activity will necessarily suppress binding to an intracellular target such as DNA. Our findings suggest that these polymers operate with a concentration-dependent mechanism of action. Polymer concentrations near the MBC allow polymer molecules to cross cell membranes and bind to DNA without complete membrane disruption. However, at polymer concentrations that significantly exceed the MBC, complete disruption of the membrane is possible.

Acknowledgments

Appendix A. Supplementary data

Supplementary data to this article can be found online at http://dx.doi.org/10.1016/j.bbamem.2014.04.007.

References

[1] R.R. Roberts, B. Hota, I. Ahmad, R.D. Scott II, S.D. Foster, F. Abbasi, S. Schabowski, L.M. Kampe, G.G. Ciavarella, M. Supino, J. Naples, R. Cordell, S.B. Levy, R.A. Weinstein, Hospital and societal costs of antimicrobial-resistant infections in a Chicago teaching hospital: implications for antibiotic stewardship, Clin. Infect. Dis. 49 (2009) 1175–1184.
[2] J.G. Hurdle, A.J. O'Neill, I. Chopra, R.E. Lee, Targeting bacterial membrane function: an underexploited mechanism for treating persistent infections, Nat. Rev. Microbiol. 9 (2011) 62–75.
[3] I. Chopra, L. Hesse, A.J. O'Neill, Exploiting current understanding of antibiotic action for discovery of new drugs, J. Appl. Microbiol. 92 (2002) 4S–15S (Suppl.).
[4] B.R. Levin, D.E. Rozen, Non-inherited antibiotic resistance, Nat. Rev. Microbiol. 4 (2006) 556–562.
[5] A.R.M. Coates, Y. Hu, Targeting non-multiplying organisms as a way to develop novel antimicrobials, Trends Pharmacol. Sci. 29 (2008) 143–150.
[6] R.E.W. Hancock, H.-G. Sahl, Antimicrobial and host-defense peptides as new anti-infective therapeutic strategies, Nat. Biotechnol. 24 (2006) 1551–1557.
[7] N.W. Schmidt, A. Mishra, G.H. Lai, M. Davis, L.K. Sanders, D. Tran, A. Garcia, K.P. Tai, P.B. McCray, A.J. Ouellette, M.E. Selsted, G.C. Wong, Criterion for amino acid composition of defensins and antimicrobial peptides based on geometry of membrane destabilization, J. Am. Chem. Soc. 133 (2011) 6720–6727.
[8] M. Zasloff, Antimicrobial peptides of multicellular organisms, Nature 415 (2002) 389–395.
[9] K.A. Brogden, Antimicrobial peptides: pore formers or metabolic inhibitors in bacteria? Nat. Rev. Microbiol. 3 (2005) 238–250.
[10] Y. Shai, Mechanism of the binding, insertion and destabilization of phospholipid bilayer membranes by α-helical antimicrobial and cell non-selective membrane-lytic peptides, Biochim. Biophys. Acta Biomembr. 1462 (1999) 55–70.
[11] A.K. Marr, W.J. Gooderham, R.E.W. Hancock, Antibacterial peptides for therapeutic use: obstacles and realistic outlook, Curr. Opin. Pharmacol. 6 (2006) 468–472.
[12] U.H.N. Dürr, U.S. Sudheendra, A. Ramamoorthy, LL-37, the only human member of the cathelicidin family of antimicrobial peptides, Biochim. Biophys. Acta Biomembr. 1758 (2006) 1408–1425.
[13] H. Steiner, D. Hultmark, A. Engstrom, H. Bennich, H.G. Boman, Sequence and specificity of two antibacterial proteins involved in insect immunity, Nature 292 (1981) 246–248.
[14] M. Zasloff, Magainins, a class of antimicrobial peptides from Xenopus skin: isolation, characterization of two active forms, and partial cDNA sequence of a precursor, Proc. Natl. Acad. Sci. U. S. A. 84 (1987) 5449–5453.
[15] S. Chakraborty, R. Liu, J.J. Lemke, Z. Hayouka, R.A. Welch, B. Weisblum, K.S. Masters, S.H. Gellman, Effects of cyclic vs. acyclic hydrophobic subunits on the chemical structure and biological properties of nylon-3 co-polymers, ACS Macro Lett. 2 (2013).
[16] K. Matsuzaki, Why and how are peptide–lipid interactions utilized for self-defense? Magainins and tachyplesins as archetypes, Biochim. Biophys. Acta Biomembr. 1462 (1999) 1–10.
[17] K. Matsuzaki, K.-i. Sugishita, N. Ishibe, M. Ueha, S. Nakata, K. Miyajima, R.M. Epand, Relationship of membrane curvature to the formation of pores by magainin 2, Biochemistry 37 (1998) 11856–11863.
[18] H.W. Huang, Action of antimicrobial peptides: two-state model, Biochemistry 39 (2000) 8347–8352.
[19] L. Yang, V.D. Gordon, D.R. Trinkle, N.W. Schmidt, M.A. Davis, C. DeVries, A. Som, J.E. Cronan Jr., G.N. Tew, G.C. Wong, Mechanism of a prototypical synthetic membrane-active antimicrobial: efficient hole-punching via interaction with negative intrinsic curvature lipids, Proc. Natl. Acad. Sci. U. S. A. 105 (2008) 20595–20600.
[20] L. Yang, V.D. Gordon, A. Mishra, A. Som, K.R. Purdy, M.A. Davis, G.N. Tew, G.C.L. Wong, Synthetic antimicrobial oligomers induce a composition-dependent topological transition in membranes, J. Am. Chem. Soc. 129 (2007) 12141–12147.
[21] N.J. Afacan, A.T. Yeung, O.M. Pena, R.E. Hancock, Therapeutic potential of host defense peptides in antibiotic-resistant infections, Curr. Pharm. Des. 18 (2012) 807–819.
[22] C. Vilhena, A. Bettencourt, Daptomycin: a review of properties, clinical use, drug delivery and resistance, Mini-Rev. Med. Chem. 12 (2012) 202–209.

[23] L. Zhou, X.-H. Lei, B.R. Bochner, B.L. Wanner, Phenotype microarray analysis of *Escherichia coli* K-12 mutants with deletions of all two-component systems, J. Bacteriol. 185 (2003) 4956–4972.

[24] M. Matsuo, F. Kato, Y. Oogai, T. Kawai, M. Sugai, H. Komatsuzawa, Distinct two-component systems in methicillin-resistant *Staphylococcus aureus* can change the susceptibility to antimicrobial agents, J. Antimicrob. Chemother. 65 (2010) 1536–1537.

[25] M.W. Bader, S. Sanowar, M.E. Daley, A.R. Schneider, U. Cho, W. Xu, R.E. Klevit, H. Le Moual, S.I. Miller, Recognition of antimicrobial peptides by a bacterial sensor kinase, Cell 122 (2005) 461–472.

[26] C.M. Ernst, A. Peschel, Broad-spectrum antimicrobial peptide resistance by MprF-mediated aminoacylation and flipping of phospholipids, Mol. Microbiol. 80 (2011) 290–299.

[27] D.J. Farrell, M. Robbins, W. Rhys-Williams, W.G. Love, Investigation of the potential for mutational resistance to XF-73, retapamulin, mupirocin, fusidic acid, daptomycin, and vancomycin in methicillin-resistant *Staphylococcus aureus* isolates during a 55-passage study, Antimicrob. Agents Chemother. 55 (2011) 1177–1181.

[28] R.E.W. Hancock, J.B. McPhee, Salmonella's sensor for host defense molecules, Cell 122 (2005) 320–322.

[29] T. Koprivnjak, A. Peschel, Bacterial resistance mechanisms against host defense peptides, Cell. Mol. Life Sci. 68 (2011) 2243–2254.

[30] T. Koprivnjak, D. Zhang, C.M. Ernst, A. Peschel, W.M. Nauseef, J.P. Weiss, Characterization of *Staphylococcus aureus* cardiolipin synthases 1 and 2 and their contribution to accumulation of cardiolipin in stationary phase and within phagocytes, J. Bacteriol. 193 (2011) 4134–4142.

[31] J.B. McPhee, M. Bains, G. Winsor, S. Lewenza, A. Kwasnicka, M.D. Brazas, F.S.L. Brinkman, R.E.W. Hancock, Contribution of the PhoP-PhoQ and PmrA-PmrB two-component regulatory systems to Mg^{2+}-induced gene regulation in *Pseudomonas aeruginosa*, J. Bacteriol. 188 (2006) 3995–4006.

[32] V. Nizet, Antimicrobial peptide resistance mechanisms of human bacterial pathogens, Curr. Issues Mol. Biol. 8 (2006) 11–26.

[33] A. Rubio, M. Conrad, R.J. Haselbeck, G.C. Kedar, V. Brown-Driver, J. Finn, J.A. Silverman, Regulation of mprF by antisense RNA restores daptomycin susceptibility to daptomycin-resistant isolates of *Staphylococcus aureus*, Antimicrob. Agents Chemother. 55 (2011) 364–367.

[34] S. Fernandez-Lopez, H.S. Kim, E.C. Choi, M. Delgado, J.R. Granja, A. Khasanov, K. Kraehenbuehl, G. Long, D.A. Weinberger, K.M. Wilcoxen, M.R. Ghadiri, Antibacterial agents based on the cyclic D,L-alpha-peptide architecture, Nature 412 (2001) 452–455.

[35] H.S. Won, S.J. Jung, H.E. Kim, M.D. Seo, B.J. Lee, Systematic peptide engineering and structural characterization to search for the shortest antimicrobial peptide analogue of gaegurin 5, J. Biol. Chem. 279 (2004) 14784–14791.

[36] Y. Chen, C.T. Mant, S.W. Farmer, R.E. Hancock, M.L. Vasil, R.S. Hodges, Rational design of alpha-helical antimicrobial peptides with enhanced activities and specificity/therapeutic index, J. Biol. Chem. 280 (2005) 12316–12329.

[37] D. Liu, W.F. DeGrado, De novo design, synthesis, and characterization of antimicrobial β-peptides, J. Am. Chem. Soc. 123 (2001) 7553–7559.

[38] E.A. Porter, X. Wang, H.-S. Lee, B. Weisblum, S.H. Gellman, Antibiotics: non-haemolytic β-amino-acid oligomers, Nature 404 (2000) 565.

[39] E.A. Porter, B. Weisblum, S.H. Gellman, Mimicry of host-defense peptides by unnatural oligomers: antimicrobial beta-peptides, J. Am. Chem. Soc. 124 (2002) 7324–7330.

[40] Y. Hamuro, J.P. Schneider, W.F. DeGrado, De novo design of antibacterial β-peptides, J. Am. Chem. Soc. 121 (1999) 12200–12201.

[41] M.A. Schmitt, B. Weisblum, S.H. Gellman, Unexpected relationships between structure and function in α,β-peptides: antimicrobial foldamers with heterogeneous backbones, J. Am. Chem. Soc. 126 (2004) 6848–6849.

[42] M.A. Schmitt, B. Weisblum, S.H. Gellman, Interplay among folding, sequence, and lipophilicity in the antibacterial and hemolytic activities of α/β-peptides, J. Am. Chem. Soc. 129 (2007) 417–428.

[43] J.A. Patch, A.E. Barron, Helical peptoid mimics of magainin-2 amide, J. Am. Chem. Soc. 125 (2003) 12092–12093.

[44] D. Liu, S. Choi, B. Chen, R.J. Doerksen, D.J. Clements, J.D. Winkler, M.L. Klein, W.F. DeGrado, Nontoxic membrane-active antimicrobial arylamide oligomers, Angew. Chem. Int. Ed. Engl. 43 (2004) 1158–1162.

[45] H. Tang, R.J. Doerksen, T.V. Jones, M.L. Klein, G.N. Tew, Biomimetic facially amphiphilic antibacterial oligomers with conformationally stiff backbones, Chem. Biol. 13 (2006) 427–435.

[46] G.N. Tew, D. Clements, H. Tang, L. Arnt, R.W. Scott, Antimicrobial activity of an abiotic host defense peptide mimic, Biochim. Biophys. Acta Biomembr. 1758 (2006) 1387–1392.

[47] G.N. Tew, D. Liu, B. Chen, R.J. Doerksen, J. Kaplan, P.J. Carroll, M.L. Klein, W.F. DeGrado, De novo design of biomimetic antimicrobial polymers, Proc. Natl. Acad. Sci. U. S. A. 99 (2002) 5110–5114.

[48] L. Arnt, K. Nüsslein, G.N. Tew, Nonhemolytic abiogenic polymers as antimicrobial peptide mimics, J. Polym. Sci. A Polym. Chem. 42 (2004) 3860–3864.

[49] K. Hu, N.W. Schmidt, R. Zhu, Y. Jiang, G.H. Lai, G. Wei, E.F. Palermo, K. Kuroda, G.C. Wong, L. Yang, A critical evaluation of random copolymer mimesis of homogeneous antimicrobial peptides, Macromolecules 46 (2013) 1908–1915.

[50] M.A. Gelman, B. Weisblum, D.M. Lynn, S.H. Gellman, Biocidal activity of polystyrenes that are cationic by virtue of protonation, Org. Lett. 6 (2004) 557–560.

[51] B.P. Mowery, S.E. Lee, D.A. Kissounko, R.F. Epand, R.M. Epand, B. Weisblum, S.S. Stahl, S.H. Gellman, Mimicry of antimicrobial host-defense peptides by random copolymers, J. Am. Chem. Soc. 129 (2007) 15474–15476.

[52] R.F. Epand, B.P. Mowery, S.E. Lee, S.S. Stahl, R.I. Lehrer, S.H. Gellman, R.M. Epand, Dual mechanism of bacterial lethality for a cationic sequence-random copolymer that mimics host-defense antimicrobial peptides, J. Mol. Biol. 379 (2008) 38–50.

[53] B.P. Mowery, A.H. Lindner, B. Weisblum, S.S. Stahl, S.H. Gellman, Structure–activity relationships among random nylon-3 copolymers that mimic antibacterial host-defense peptides, J. Am. Chem. Soc. 131 (2009) 9735–9745.

[54] K. Lienkamp, A.E. Madkour, A. Musante, C.F. Nelson, K. Nüsslein, G.N. Tew, Antimicrobial polymers prepared by ROMP with unprecedented selectivity: a molecular construction kit approach, J. Am. Chem. Soc. 130 (2008) 9836–9843.

[55] E.F. Palermo, S. Vemparala, K. Kuroda, Cationic spacer arm design strategy for control of antimicrobial activity and conformation of amphiphilic methacrylate random copolymers, Biomacromolecules 13 (2012) 1632–1641.

[56] J. Zhang, D.A. Kissounko, S.E. Lee, S.H. Gellman, S.S. Stahl, Access to poly-β-peptides with functionalized side chains and end groups via controlled ring-opening polymerization of β-lactams, J. Am. Chem. Soc. 131 (2009) 1589–1597.

[57] A. Som, L. Yang, G.C. Wong, G.N. Tew, Divalent metal ion triggered activity of a synthetic antimicrobial in cardiolipin membranes, J. Am. Chem. Soc. 131 (2009) 15102–15103.

[58] R.M. Bell, R.D. Mavis, P.R. Vagelos, Altered phospholipid metabolism in a temperature-sensitive mutant of *Escherichia coli*, $CR_{34}T_46$, Biochim. Biophys. Acta 270 (1972) 504–512.

[59] S. Clejan, T.A. Krulwich, K.R. Mondrus, D. Seto-Young, Membrane lipid composition of obligately and facultatively alkalophilic strains of *Bacillus* spp, J. Bacteriol. 168 (1986) 334–340.

[60] R.F. Epand, P.B. Savage, R.M. Epand, Bacterial lipid composition and the antimicrobial efficacy of cationic steroid compounds (Ceragenins), Biochim. Biophys. Acta Biomembr. 1768 (2007) 2500–2509.

[61] Y. Kanemasa, T. Yoshioka, H. Hayashi, Alteration of the phospholipid composition of *Staphylococcus aureus* cultured in medium containing NaCl, Biochim. Biophys. Acta 280 (1972) 444–450.

[62] C.S. Lopez, A.F. Alice, H. Heras, E.A. Rivas, C. Sanchez-Rivas, Role of anionic phospholipids in the adaptation of *Bacillus subtilis* to high salinity, Microbiology 152 (2006) 605–616.

[63] A.G. Rietveld, J.A. Killian, W. Dowhan, B. de Kruijff, Polymorphic regulation of membrane phospholipid composition in *Escherichia coli*, J. Biol. Chem. 268 (1993) 12427–12433.

[64] M. Saint-Pierre-Chazalet, J. Plasek, I. Konopasek, A monolayer study of properties of isolated membrane phospholipids of '*Bacillus subtilis*', Colloids Surf. B: Biointerfaces 23 (2002) 43–49.

[65] Y. Sakayori, M. Muramatsu, S. Hanada, Y. Kamagata, S. Kawamoto, J. Shima, Characterization of *Enterococcus faecium* mutants resistant to mundticin KS, a class IIa bacteriocin, Microbiology 149 (2003) 2901–2908.

[66] H. Jenssen, P. Hamill, R.E.W. Hancock, Peptide antimicrobial agents, Clin. Microbiol. Rev. 19 (2006) 491–511.

[67] C.H. Hsu, C. Chen, M.L. Jou, A.Y. Lee, Y.C. Lin, Y.P. Yu, W.T. Huang, S.H. Wu, Structural and DNA-binding studies on the bovine antimicrobial peptide, indolicidin: evidence for multiple conformations involved in binding to membranes and DNA, Nucleic Acids Res. 33 (2005) 4053–4064.

[68] C.B. Park, H.S. Kim, S.C. Kim, Mechanism of action of the antimicrobial peptide buforin II: buforin II kills microorganisms by penetrating the cell membrane and inhibiting cellular functions, Biochem. Biophys. Res. Commun. 244 (1998) 253–257.

[69] K.L. Brown, R.E.W. Hancock, Cationic host defense (antimicrobial) peptides, Curr. Opin. Immunol. 18 (2006) 24–30.

[70] D.M.E. Bowdish, D.J. Davidson, M.G. Scott, R.E.W. Hancock, Immunomodulatory activities of small host defense peptides, Antimicrob. Agents Chemother. 49 (2005) 1727–1732.

[71] R. Graf, G. Lohaus, K. Börner, E. Schmidt, H. Bestian, β-Lactams, their polymerization and use as raw materials for fibers, Angew. Chem. Int. Ed. Engl. 1 (1962) 481–488.

[72] K. Hashimoto, Ring-opening polymerization of lactams. Living anionic polymerization and its applications, Prog. Polym. Sci. 25 (2000) 1411–1462.

[73] R.A. Llenado, C.S. Weeks, M.J. Cocco, A.J. Ouellette, Electropositive charge in alpha-defensin bactericidal activity: functional effects of Lys-for-Arg substitutions vary with the peptide primary structure, Infect. Immun. 77 (2009) 5035–5043.

[74] Argonne National Laboratory, Nika — package for 2D area detectors data reduction, http://usaxs.xor.aps.anl.gov/staff/ilavsky/nika.html (accessed 2013).

[75] Andy Hammersley / ESRF, The FIT2D Home Page, http://www.esrf.eu/computing/scientific/FIT2D/ (accessed 2013).

[76] C. Yanisch-Perron, J. Vieira, J. Messing, Improved M13 phage cloning vectors and host strains: nucleotide sequences of the M13mp18 and pUC19 vectors, Gene 33 (1985) 103–119.

[77] F.E. Young, C. Smith, B.E. Reilly, Chromosomal location of genes regulating resistance to bacteriophage in *Bacillus subtilis*, J. Bacteriol. 98 (1969) 1087–1097.

[78] T.I. Nicas, C.Y. Wu, J.N. Hobbs, D.A. Preston, N.E. Allen, Characterization of vancomycin resistance in *Enterococcus faecium* and *Enterococcus faecalis*, Antimicrob. Agents Chemother. 33 (1989) 1121–1124.

[79] B. Weisblum, V. Demohn, Erythromycin-inducible resistance in *Staphylococcus aureus*: survey of antibiotic classes involved, J. Bacteriol. 98 (1969) 447–452.

[80] R.I. Lehrer, A. Barton, K.A. Daher, S.S. Harwig, T. Ganz, M.E. Selsted, Interaction of human defensins with *Escherichia coli*. Mechanism of bactericidal activity, J. Clin. Invest. 84 (1989) 553–561.

[81] B. Skerlavaj, D. Romeo, R. Gennaro, Rapid membrane permeabilization and inhibition of vital functions of gram-negative bacteria by bactenecins, Infect. Immun. 58 (1990) 3724–3730.

[82] C.S. Weeks, H. Tanabe, J.E. Cummings, S.P. Crampton, T. Sheynis, R. Jelinek, T.K. Vanderlick, M.J. Cocco, A.J. Ouellette, Matrix metalloproteinase-7 activation of mouse paneth cell pro-α-defensins: SER43↓ILE44 PROTEOLYSIS ENABLES MEMBRANE-DISRUPTIVE ACTIVITY, J. Biol. Chem. 281 (2006) 28932–28942.

[83] T.J. Falla, D.N. Karunaratne, R.E.W. Hancock, Mode of action of the antimicrobial peptide indolicidin, J. Biol. Chem. 271 (1996) 19298–19303.

[84] G.S. Manning, Limiting laws and counterion condensation in polyelectrolyte solutions. I. Colligative properties, J. Chem. Phys. 51 (1969) 924–933.

[85] G.S. Manning, Counterion condensation on charged spheres, cylinders, and planes, J. Phys. Chem. B 111 (2007) 8554–8559.

[86] L.K. Sanders, W. Xian, C. Guáqueta, M.J. Strohman, C.R. Vrasich, E. Luijten, G.C.L. Wong, Control of electrostatic interactions between F-actin and genetically modified lysozyme in aqueous media, Proc. Natl. Acad. Sci. U. S. A. 104 (2007) 15994–15999.

[87] L.K. Sanders, C. Guáqueta, T.E. Angelini, J.-W. Lee, S.C. Slimmer, E. Luijten, G.C.L. Wong, Structure and stability of self-assembled actin-lysozyme complexes in salty water, Phys. Rev. Lett. 95 (2005) 108302.

[88] H.E. Kubitschek, M.L. Freedman, Chromosome replication and the division cycle of *Escherichia coli* B-r, J. Bacteriol. 107 (1971) 95–99.

[89] U.S. Schwarz, G. Gompper, Stability of inverse bicontinuous cubic phases in lipid-water mixtures, Phys. Rev. Lett. 85 (2000) 1472–1475.

[90] G.C. Shearman, O. Ces, R.H. Templer, J.M. Seddon, Inverse lyotropic phases of lipids and membrane curvature, J. Phys. Condens. Matter 18 (2006) S1105–S1124.

[91] N.W. Schmidt, M. Lis, K. Zhao, G.H. Lai, A.N. Alexandrova, G.N. Tew, G.C. Wong, Molecular basis for nanoscopic membrane curvature generation from quantum mechanical models and synthetic transporter sequences, J. Am. Chem. Soc. 134 (2012) 19207–19216.

[92] R.M. Epand, R.F. Epand, Bacterial membrane lipids in the action of antimicrobial agents, J. Pept. Sci. 17 (2011) 298–305.

[93] A. Som, G.N. Tew, Influence of lipid composition on membrane activity of antimicrobial phenylene ethynylene oligomers, J. Phys. Chem. B 112 (2008) 3495–3502.

[94] H. Liang, D. Harries, G.C. Wong, Polymorphism of DNA-anionic liposome complexes reveals hierarchy of ion-mediated interactions, Proc. Natl. Acad. Sci. U. S. A. 102 (2005) 11173–11178.

[95] A. Mishra, K.P. Tai, N.W. Schmidt, A.J. Ouellette, G.C.L. Wong, Chapter Four — Small-angle X-ray scattering studies of peptide–lipid interactions using the mouse paneth cell α-defensin cryptdin-4, in: Jo M. Holt, Michael L. Johnson, Gary K. Ackers (Eds.), Method Enzymol, vol. 492, Academic Press, 2011, pp. 127–149.

[96] W. Humphrey, A. Dalke, K. Schulten, VMD: visual molecular dynamics, J. Mol. Graph. 14 (1996) 33–38.